JOURNAL OF MATERIALS SCIENCE 22 (1987) 488-494

Computer simulation of effects of the pore size distribution on the kinetics of pressure-assisted final-stage densification

ALAN J. MARKWORTH, J. KEVIN McCOY
Battelle, 505 King Avenue, Columbus, Ohio 43201-2693, USA

Most theoretical treatments of pressure-assisted densification of porous solids assume a single size for all pores. We remove this assumption and consider a distribution of pore sizes. Dissolution of intragranular pores by volume diffusion and dissolution of intergranular pores by grain-boundary diffusion are both treated. The evolution with time of pore size distributions is calculated for distributions that are initially described by log-normal and Weibull functions, and differences in predicted behaviours are discussed. The pore size distribution is then related to two important quantities: porosity and number of pores per unit volume. The assumption of a distribution of pore sizes is found to avoid certain unrealistic predictions obtained from models with a single pore size, such as abrupt disappearance of all pores and rapid approach to full density.

1. Introduction

It is frequently observed in studies of densification that full density is difficult to achieve. This is in direct conflict with predictions of rapid and complete densification derived from theoretical models of densification by diffusion. In this paper, we show that the models can be brought into agreement with experience by consideration of the effects of a distribution of pore sizes.

The importance of size-distribution effects in considerations of the evolution of a discrete second-phase species has long been recognized. The porosity within a solid body can be regarded as a particular type of second phase, and its variation with time, resulting from surface-energy and applied-pressure driving forces, can be treated as a type of phase transformation. In this case as well, size-distribution effects can play an important role, for example in considerations of the manner in which the overall volume fraction of porosity varies with time.

Presented below are the results of a modelling study of the dissolution kinetics of a distribution of discrete (i.e. non-overlapping), spherical pores contained within a solid body. Both intragranular and intergranular pores are considered, using well-established expressions for the size-dependent rate of pore dissolution resulting from volume diffusion and grain-boundary diffusion, respectively, of vacancies away from the pore surface. The evolution with time of the pore size distribution is calculated, starting from various assumed initial distributions, and from this the corresponding variation of the overall porosity of the solid is calculated and related to size-distribution effects.

Because of the fact that both pore-surface-energy and applied-pressure driving forces are considered, the problem is not analytically tractable for either intragranular or intergranular pores. Consequently, solutions are generated numerically.

It is clear that the assumption of a system of discrete pores limits our consideration to a solid for which the amount of porosity is relatively low. This corresponds to what is commonly referred to as the "final stage" of densification. A quantitative evaluation of the probability that a given pore is actually discrete can be carried out, as, for example, has been done [1] for the case of a uniform size distribution of spheres distributed at random within three-dimensional space.

2. Pore-dissolution models

Over the years, many investigators have developed models for the growth and dissolution of pores contained within a solid body. (Actually, models for pore growth can be used to describe dissolution as well, if appropriate modification is made of the applied-stress term in the growth-rate expression, as has been discussed by Greenwood [2].) In addition, a variety of kinetic mechanisms has been considered. For purposes of the present analysis, relatively simple models for pore dissolution are used which nevertheless serve well to illustrate the manner in which size-distribution effects can influence the overall kinetics of porosity reduction.

2.1. Intragranular pores

For the volume-diffusion-controlled dissolution of an isolated, spherical, intragranular pore (i.e. neighboring pores are assumed not to influence one another), one can derive an expression for the rate of pore dissolution by assuming that the vacancy-concentration field within the solid outside the pore satisfies the Laplace equation. One thus obtains (e.g. [3, 4]),

$$\frac{dR}{dt} = -\frac{\Omega D_v}{kTR}\left(P + \frac{2\gamma}{R}\right) \quad (1)$$

0022-2461/87 $03.00 + .12 © *1987 Chapman and Hall Ltd.*

where R is the pore radius at time t; Ω, D_v and γ are the atomic volume, the volume self-diffusivity and the surface energy of the solid, respectively; P is the externally applied pressure, k is Boltzmann's constant and T is the absolute temperature. Three assumptions inherent in Equation 1 are (a) that the vacancy supersaturation in the lattice is zero, (b) that the "effective" applied pressure inside the solid is unaffected by the presence of the porosity, and (c) that no gases exist inside the pores. Relaxation of assumption (a) has been considered by Geguzin and Lifshits [3] and others; relaxation of (b) and (c) has been discussed by Markworth [4] and others.

In order to simplify the analysis which follows, we re-express Equation 1 in terms of dimensionless variables, i.e. a pore-size parameter ϱ and a time parameter τ defined as

$$\varrho \equiv \left(\frac{P}{2\gamma}\right) R \tag{2}$$

$$\tau \equiv \left(\frac{\Omega D_v P^3}{4\gamma^2 kT}\right) t \tag{3}$$

in terms of which Equation 1 assumes the much simpler form

$$\frac{d\varrho}{d\tau} = -\frac{1}{\varrho}\left(1 + \frac{1}{\varrho}\right) \tag{4}$$

2.2. Intergranular pores

A number of models have been developed with which to describe the grain-boundary diffusion-controlled and volume-diffusion-controlled growth or dissolution of an intergranular pore. For the present analysis, we consider an isolated spherical pore situated on a planar grain boundary and dissolving by the flow of vacancies away from the pore through the boundary. To describe this situation, we apply a model for grain-boundary-diffusion controlled *growth* of an intergranular pore developed by Trinkaus [5]. The above-noted modification suggested by Greenwood [2] is used to adapt the model to pore-dissolution kinetics. One thus obtains

$$\frac{dR}{dt} = -\frac{\Omega D_b \delta}{2kTR^2}\left(P + \frac{2\gamma}{R}\right) \tag{5}$$

where D_b is the grain-boundary self-diffusivity, δ is the effective thickness of the grain boundary, and all other symbols are as defined for Equation 1. Again, it is assumed that the "effective" applied pressure inside the solid is unaffected by the presence of porosity and that no gases exist inside the pores. Effects of gases inside the pores could be considered [5] and are analogous the corresponding effects for intragranular pores.

It is again convenient to express Equation 5 in terms of dimensionless variables. We use the same size and time parameters, ϱ and τ, given by Equations 2 and 3, but we define a new dimensionless factor, α, as

$$\alpha = \frac{P\delta}{4\gamma}\frac{D_b}{D_v} \tag{6}$$

and obtain the following simpler form for Equation 5:

$$\frac{d\varrho}{d\tau} = -\frac{\alpha}{\varrho^2}\left(1 + \frac{1}{\varrho}\right) \tag{7}$$

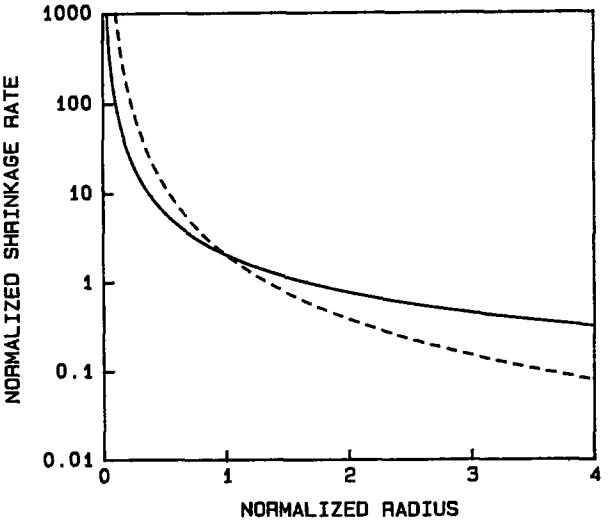

Figure 1 Normalized shrinkage rate as a function of normalized pore radius for two types of pores. (——) intragranular pores, (– – –) intergranular pores.

The rate of pore shrinkage $-d\varrho/d\tau$ as a function of pore radius ϱ is plotted in Fig. 1 for both intergranular and intragranular pores, as calculated from Equations 4 and 7 with a value of $\alpha = 1$. From Fig. 1, it can be seen that the rate of pore shrinkage decreases as pore radius increases, and that the dependence of shrinkage rate on pore size is stronger for intergranular pores than it is for intragranular pores. Note that the shrinkage rate for intergranular pores is dependent on α, and that the corresponding curve in Fig. 1 would be raised or lowered if a different value of α had been chosen.

2.3. Other pore-dissolution models

Clearly, pore-dissolution models other than those represented by Equations 4 and 7 could have been used. These two particular models were chosen because they are particularly amenable to the size-distribution analyses developed below while still containing a description of some essential features of the physics of the respective dissolution processes.

One interesting case not mentioned above is the oft-quoted model of Hull and Rimmer [6] for the stress-induced growth of grain-boundary voids. Using their model, and including only applied-pressure and surface-energy effects as driving forces for pore dissolution, one obtains an expression equivalent to Equation 4 as the dimensionless representation, noting that Equation 4 was derived for a model of *intragranular* pores. The only difference would be the replacement of D_v in Equation 1 with $D_b\delta/2a$ where a is the mean separation between pores. Consequently, the analysis of intragranular porosity based on Equation 1 is mathematically equivalent to that of intergranular porosity based on the Hull–Rimmer model [6]. It should be noted however, that important corrections to the Hull–Rimmer model have been made, e.g. by Weertman [7].

3. Size-distribution kinetics

3.1. Evolution of the pore size distribution

We define the size-distribution function for a system of pores as $f(R, t)$, such that $f(R, t)dR$ is the

concentration of pores, at time t, having radius within the range R to $R + dR$. Clearly, it is assumed in this definition that the size distribution exhibits no spatial dependence, on the average. Assuming that no "sources" or "sinks" for pores exist, one can show that the function f satisfies the following continuity relation:

$$\frac{\partial f}{\partial t} + \frac{\partial}{\partial R}(vf) = 0 \tag{8}$$

where v is a function that describes the rate at which a given pore, which can be considered as a point existing in a one-dimensional pore-radius space, moves through that space. (Obviously, the definition of v is equivalent to dR/dt which is given in Equations 1 and 5 for the two models under consideration here.) Expressing Equation 8 in terms of the dimensionless parameters ϱ and τ,

$$\frac{\partial f}{\partial \tau} + \frac{\partial}{\partial \varrho}(vf) = 0 \tag{9}$$

where now $f(\varrho, \tau)d\varrho$ is the concentration of pores, at time τ having radius within the range ϱ to $\varrho + d\varrho$, and v is now equivalent to the "velocity", $d\varrho/d\tau$, in ϱ-space.

The "flux" of pores crossing a given point of the one-dimensional ϱ-space is, in general, equal to $v(\varrho, \tau)f(\varrho, \tau)$. For the pore-dissolution models under consideration here, v has explicit dependence only upon ϱ (see Equations 4 and 7).

Let us examine the behaviour of the pore flux with respect to a *moving* coordinate frame in our one-dimensional ϱ-space. Specifically, let ϱ' be a coordinate which moves along the ϱ-axis at the same rate as a pore having instantaneous size ϱ. Hence, ϱ' is given through the relation

$$\tau - \tau_0 = \int_{\varrho_0}^{\varrho'} \frac{d\varrho}{v(\varrho)} \tag{10}$$

where ϱ_0 is the size of the pore at some given initial time τ_0 and where we again take v to depend only upon ϱ. From Equation 10 we obtain

$$\frac{d\varrho'}{d\tau} = v(\varrho') \tag{11}$$

It now follows that

$$\frac{d}{d\tau}[v(\varrho')f(\varrho', \tau)] = \left[\frac{dv(\varrho')}{d\varrho'}\frac{d\varrho'}{d\tau}\right] f(\varrho', \tau) + v(\varrho')\left[\frac{\partial}{\partial \varrho'} f(\varrho', \tau)\frac{d\varrho'}{d\tau} + \frac{\partial}{\partial \tau} f(\varrho', \tau)\right] \tag{12}$$

Combining Equations 11 and 12,

$$\frac{d}{d\tau}[v(\varrho')f(\varrho', \tau)] = v(\varrho')\left[\frac{dv(\varrho')}{d\varrho'} f(\varrho', \tau) + v(\varrho')\frac{\delta}{\delta \varrho'} f(\varrho', \tau) + \frac{\partial}{\partial \tau} f(\varrho', \tau)\right] \tag{13}$$

Now, the continuity equation, Equation 9, must also be satisfied with respect to the moving coordinate system, in which case the sum of the terms within brackets on the right hand side of Equation 13 is zero. Consequently,

$$\frac{d}{d\tau}[v(\varrho')f(\varrho', \tau)] = 0 \tag{14}$$

An alternative way of expressing Equation 14 is the following:

$$v(\varrho)f(\varrho, \tau) = v(\varrho_0)f(\varrho_0, \tau_0) \tag{15}$$

where ϱ (dropping the prime symbol) is understood to be the size of a pore, at time τ, that had size ϱ_0 at an earlier time τ_0. Taking $\tau_0 = 0$ and $g(\varrho_0) \equiv f(\varrho_0, 0)$, we obtain

$$f(\varrho, \tau) = \left[\frac{v(\varrho_0)}{v(\varrho)}\right] g(\varrho_0) \tag{16}$$

Equation 16 can be used to relate the size distribution at time $\tau = 0$ to that at some late time $\tau > 0$. An alternative derivation of Equation 15 is presented in the Appendix.

In order to apply Equation 16 to cases of interest here, one can use Equation 10 (again, and from now on, dropping the prime symbol) together with the given expressions for $v(\varrho)$. This can be done in closed form for the models under consideration here. In particular, substituting the right-hand side of Equation 4 for $v(\varrho)$ into Equation 10 and integrating, one obtains the following expression for intragranular pores:

$$\tau = \tfrac{1}{2}(\varrho_0 - \varrho)(\varrho_0 + \varrho - 2) + \ln\left(\frac{1 + \varrho_0}{1 + \varrho}\right) \tag{17}$$

Likewise, substituting the right-hand side of Equation 7 for $v(\varrho)$ into Equation 10 and integrating, one obtains the following expression for intergranular pores:

$$\alpha\tau = \tfrac{1}{3}(\varrho_0^3 - \varrho^3) + (\varrho_0 - \varrho) - \tfrac{1}{2}(\varrho_0^2 - \varrho^2) + \ln\left(\frac{1 + \varrho}{1 + \varrho_0}\right) \tag{18}$$

Unfortunately, for given values of τ and ϱ_0, the value of ϱ can be calculated from either Equation 17 or 18 only through some numerical procedure. Given this fact, however, the problem of calculating the evolution of the pore size distribution is, in principle, solved.

The above analysis can be cast in somewhat simpler form by taking

$$\varrho_0 = \varrho + \Delta \tag{19}$$

where $\Delta > 0$ since the pores are dissolving. In this form, Equations 16, 17 and 18, respectively, become

$$f(\varrho, \tau) = \frac{v(\varrho + \Delta)}{v(\varrho)} g(\varrho + \Delta) \tag{20}$$

$$\tau = \Delta(\varrho - 1 + \tfrac{1}{2}\Delta) + \ln\left(\frac{1 + \varrho + \Delta}{1 + \varrho}\right) \tag{21}$$

$$\alpha\tau = \Delta(\varrho^2 + \varrho\Delta + \tfrac{1}{3}\Delta^2 + 1 - \varrho - \tfrac{1}{2}\Delta) - \ln\left(\frac{1 + \varrho + \Delta}{1 + \varrho}\right) \tag{22}$$

For given ϱ and τ, Equations 21 and 22 can be solved numerically for the corresponding values of Δ for intragranular and intergranular pores, respectively.

3.2. Evolution of distribution-function moments

Properties of physical interest are related to moments of the size-distribution function, rather than to the distribution function *per se*, defining the ith algebraic moment (i.e. the ith moment about $\varrho = 0$) as

$$M_i(\tau) = \int_0^\infty \varrho^i f(\varrho, \tau)\, d\varrho \qquad (23)$$

For example, $M_0(\tau)$ is the net concentration of pores within the solid, and the volume fraction occupied by porosity is linearly proportional to $M_3(\tau)$.

There are different ways in which $M_i(\tau)$ can be calculated (e.g. [8, 9]). As discussed below, the approach used here is to calculate $f(\varrho, \tau)$ using a general approach described above, and then numerically integrating, using Equation 23 as a basis, to determine the moments of interest.

One case is of particular interest, namely that involving M_0. It can easily be shown that an alternative expression for M_0 is

$$M_0(\tau) = \int_{\Delta_0}^\infty g(\varrho)\, d\varrho \qquad (24)$$

where the quantity Δ_0 in Equation 24 is the value of Δ, obtained from Equation 21 or 22, corresponding to $\varrho = 0$. Thus, for intragranular and intergranular pores, respectively,

$$\tau = \Delta_0(\tfrac{1}{2}\Delta_0 - 1) + \ln(1 + \Delta_0) \qquad (25)$$

$$\alpha\tau = \Delta_0(\tfrac{1}{3}\Delta_0^2 - \tfrac{1}{2}\Delta_0 + 1) - \ln(1 + \Delta_0) \qquad (26)$$

The values of M_0 can be calculated, for a given value of τ, simply by numerically determining the pertinent value of Δ_0 from Equation 25 or 26, and then performing the integration indicated in Equation 24. The result obtained by this approach should yield the same result as that obtained from the approach previously described based on the use of Equation 23. In fact, comparison of the values of M_0 calculated using the two different approaches would serve as a useful check of the accuracy of the numerical procedures and was indeed used for this purpose in the examples described below.

4. Application to specific examples

The methods of calculating size-distrubution kinetics described above may be applied to a wide variety of inital pore-size distributions. We have applied them to a Weibull distribution

$$g(\varrho) = m\varrho^{m-1} \exp(-\varrho^m) \qquad (25)$$

with $m = 2$, 2.5, and 3, and to a log-normal distribution

$$g(\varrho) = \frac{1}{(2\pi)^{1/2} c\varrho} \exp\left(\frac{-[\ln(\varrho/b)]^2}{2c^2}\right) \qquad (26)$$

where we have taken $b = 0.8$ and $c = 0.5$. As will be seen from the figures below, these distributions are generally similar in appearance. The most important difference among them is that the log-normal distribution has a long large-radius tail, while the large-radius tails of the Weibull distrubutions are smaller and decrease with increasing m.

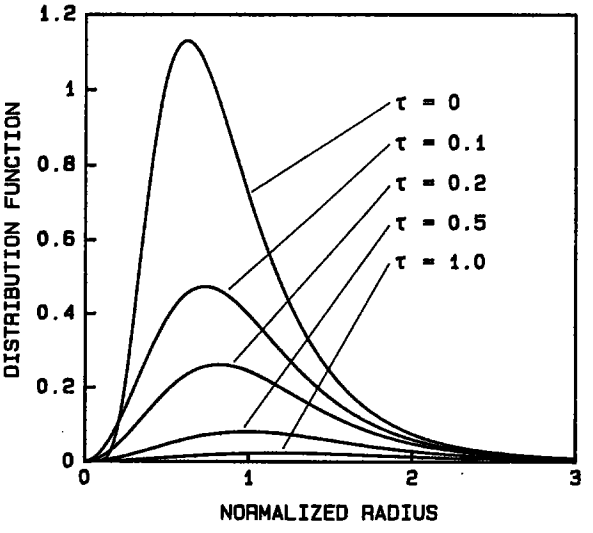

Figure 2 Pore size distribution function for intragranular pores at several times. Initial distribution is log-normal.

All of these functions are normalized, that is they have $M_0 = 1$. However, due to the differences between the functions, it is generally not possible to normalize the third moments simultaneously. For the Weibull distributions, we have $M_3 = \Gamma(1 + 3/m)$ while for the log-normal distribution, $M_3 = b^3 \exp(9c^2/2)$.

In Figs 2 to 4 we present plots of the pore size distribution function for selected times and various initial distributions as calculated using Equation 4 for the kinetics of dissolution of intragranular pores. Results for the Weibull distribution with $m = 2.5$ are not plotted but were intermediate between the results for $m = 2$ and $m = 3$. From Fig. 2, it will be noted that the position of the peak of the distribution function moves toward larger radii as time progresses. A similar but smaller effect can be seen in Fig. 3, while in Fig. 4, the position of the peak clearly shifts toward smaller radii. This behaviour is in marked contrast to that of standard models in which all pores are the

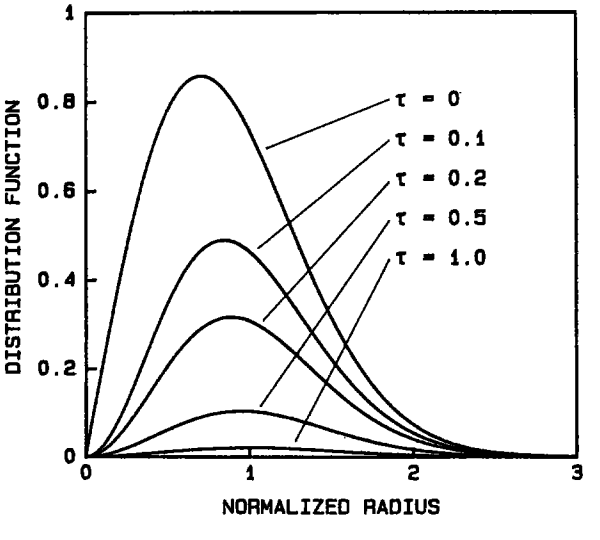

Figure 3 Pore size distribution function for intragranular pores at several times. Initial distribution is Weibull with $m = 2$.

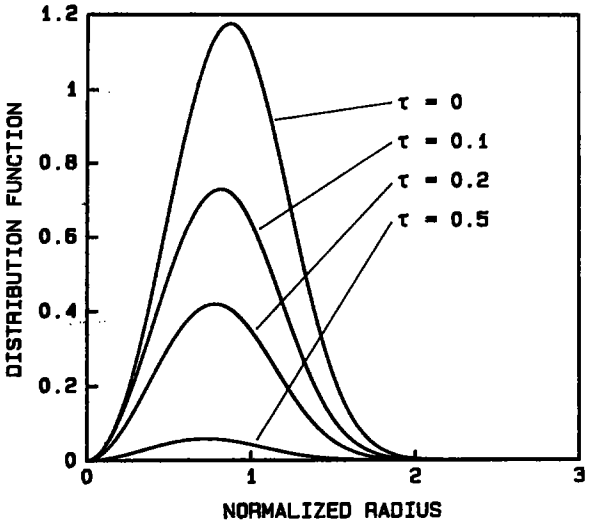

Figure 4 Pore size distribution function for intragranular pores at several times. Initial distribution is Weibull with $m = 3$.

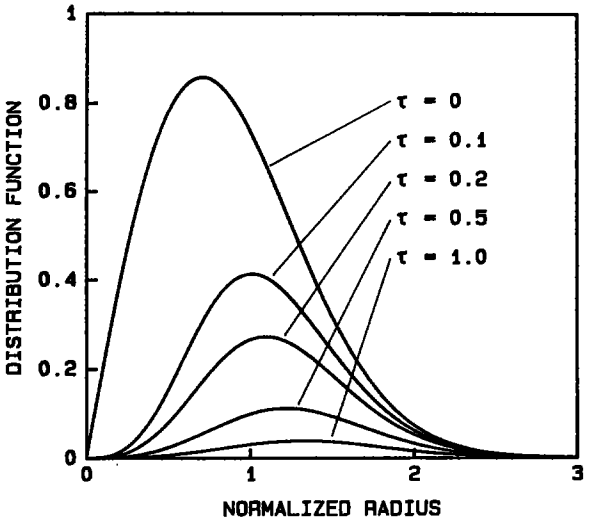

Figure 6 Pore size distribution function for intergranular pores at several times. Initial distribution is Weibull with $m = 2$.

same size and all pores shrink together: for densification to occur, the pore radius must shrink. If there is a distribution of pore sizes, however, the peak of the distribution may move in either direction, depending on the shape of the distribution and the velocity function. The influence of the velocity function may be seen in Figs 5 to 7, which differ from Figs 2 to 4 only in that the velocity for intergranular pores was used. For all calculations with intergranular pores we took $\alpha = 1$. As seen in Figs 5 to 7, the peak shifts strongly to higher radii for the log-normal distribution, somewhat less strongly for the Weibull distribution with $m = 2$, and only slightly for the Weibull distribution with $m = 3$. It is clear from the figures that, qualitatively, if the magnitude of the velocity function decreases strongly with increasing radius and the initial distribution has a long large-radius tail, the peak of the distribution function will shift toward the right, since the small pores disappear quickly, leaving the larger pores almost unchanged. Conversely, if the velocity function depends weakly on radius and the initial distribution is narrow, the pores will shrink together and the peak of the distribution will move to the left.

While the pore size distribution functions would be difficult to determine experimentally, two quantities that are more easily measured are the number of pores per unit volume and the porosity. These two quantities are proportional to M_0 and M_3, respectively. The moments are plotted as functions of time for all four distributions and both velocity functions in Figs 8 to 11. For comparison, we have also plotted the third moments for a distribution in which all pores are the same size. An initial pore radius of $\varrho = (3/4\pi)^{1/3}$ was used.

If it is assumed that all pores have the same size, all pores vanish simultaneously, and M_0 changes discontinuously. A more realistic picture is seen in Figs 8 and 10: the number of pores gradually decreases toward zero. At times up to $\tau = 0.2$, the number of pores decreases at comparable rates for all four distributions, reflecting the general similarity of the central portion of the distributions. By $\tau = 1$, however, the distributions are dominated by what was originally the large-radius tail of the distribution, and, for both velocity functions, the log-normal distribution has the largest number of pores, followed by the Weibull distributions in order of increasing m.

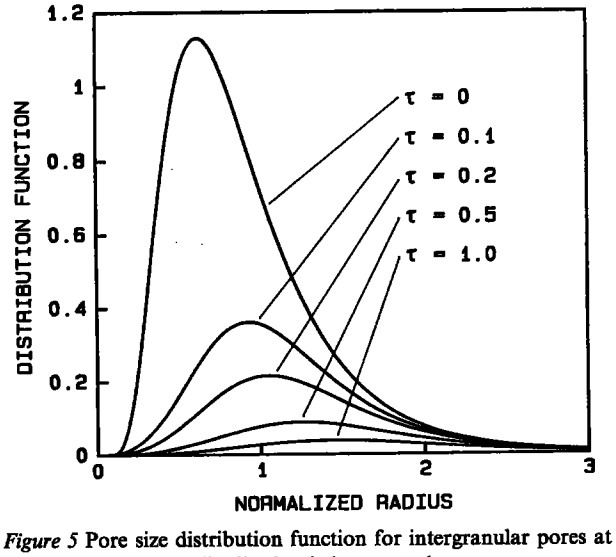

Figure 5 Pore size distribution function for intergranular pores at several times. Initial distribution is log-normal.

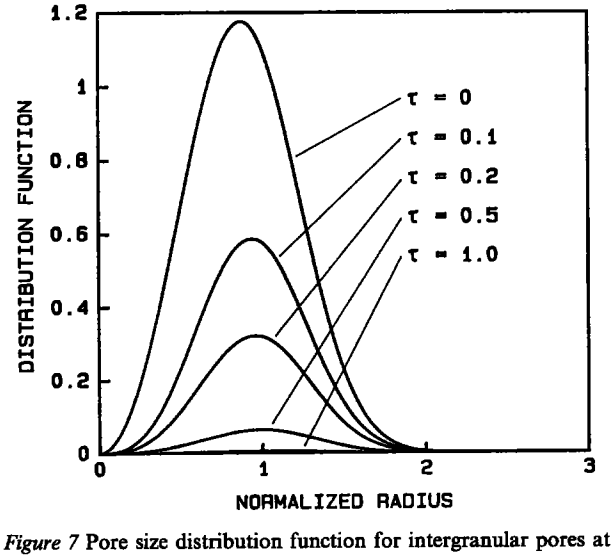

Figure 7 Pore size distribution function for intergranular pores at several times. Initial distribution is Weibull with $m = 3$.

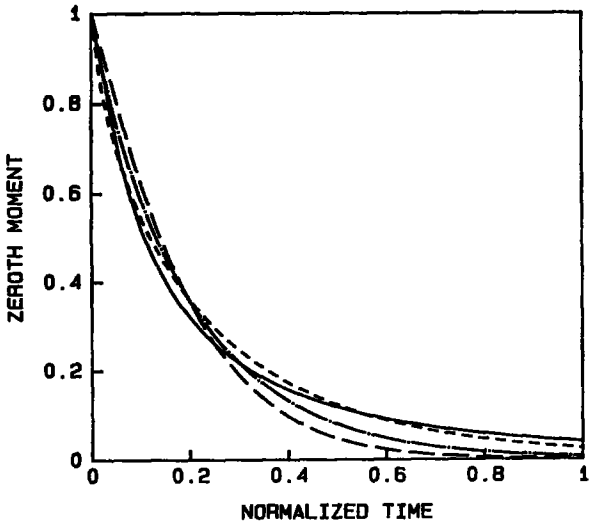

Figure 8 Zeroth moment of the pore distribution function (proportional to number of pores) as a function of time for intragranular pores with four initial pore size distributions: (——) log-normal; (– – –) Weibull, $m = 2$; (–·–) Weibull, $m = 2.5$; (— —) Weibull, $m = 3$.

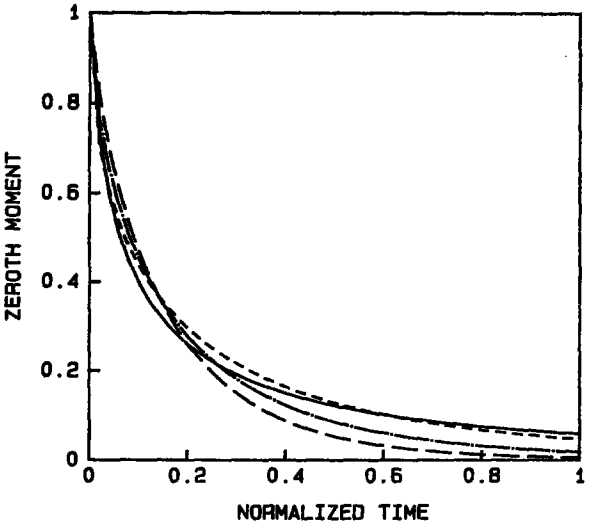

Figure 10 Zeroth moment of the pore distribution function (proportional to number of pores) as a function of time for intragranular pores with four initial pore size distributions: (——) log-normal; (– – –) Weibull, $m = 2$; (–·–) Weibull, $m = 2.5$; (— —) Weibull, $m = 3$.

From Figs 9 and 11, we note again the unrealistic results obtained by assuming a single pore size: densification proceeds rapidly to completion. At short times, the rates of change of the third moment as obtained by assuming a distribution of pore sizes agree relatively well with those for a single pore size and with each other. However, the results soon begin to diverge. For a single size of intragranular pores, it is predicted that all porosity will vanish at $\tau = 0.247$, but all the calculations with a distribution of sizes give significant remaining porosity at this time. The contrast is even stronger in the case of intergranular pores. The calculation with a single pore size shows all porosity vanishing at $\tau = 0.196$, but, for the log-normal distribution and Weibull distribution with $m = 2$, more than half of the original porosity remains. For both velocity functions, the calculations on a log-normal distribution give significant remaining porosity at $\tau = 1$.

5. Discussion

Size-distribution effects associated with pores in solids have been studied by other investigators as well. For example, Tomandl [10] considered pore shrinkage resulting from sintering without any externally applied pressure. The expression he used to describe the rate of pore dissolution by diffusion along grain boundaries was

$$\frac{dR}{dt} = -\frac{c_p}{R^2} \tag{27}$$

where c_p is a parameter that is dependent upon temperature. Clearly, Equation 27 is mathematically equivalent to Equation 1 if P is set equal to zero in the latter. They then differ only in the form of the coefficient of the R^{-2} term. For this limiting case, the time-dependent size-distribution function can be derived in closed form, as Tomandl has shown [10]. In other studies [11, 12], the evolution of a cavity size

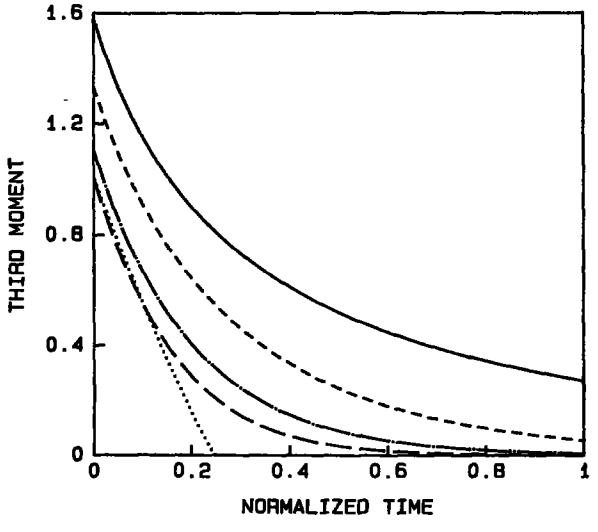

Figure 9 Third moment of the pore distribution function (proportional to porosity) as a function of time for intragranular pores with five initial pore size distributions: (——) log-normal; (– – –) Weibull, $m = 2$; (–·–) Weibull, $m = 2.5$; (— —) Weibull, $m = 3$; (· · ·) single pore size.

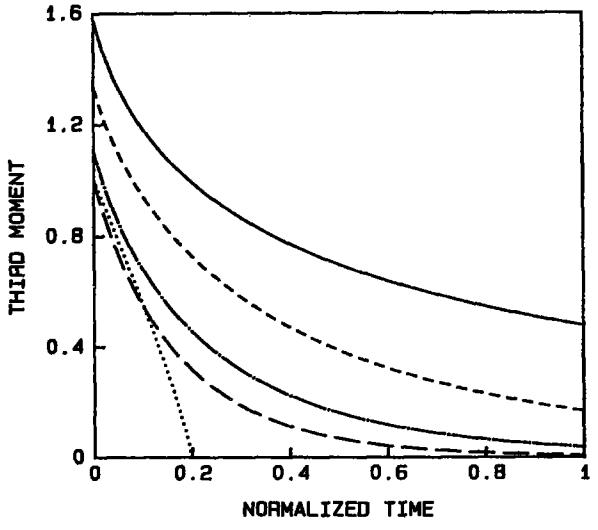

Figure 11 Third moment of the pore distribution function (proportional to porosity) as a function of time for intragranular pores with five initial pore size distributions: (——) log-normal; (– – –) Weibull, $m = 2$; (–·–) Weibull, $m = 2.5$; (— —) Weibull, $m = 3$; (· · ·) single pore size.

distribution under an applied tensile stress was studied. The rate of change of pore size was here described by an expression equivalent to our Equation 5, with P replaced with $-\sigma$, where σ is the tensile stress at and perpendicular to the grain boundary. It was assumed that σ is equal to the externally applied tensile stress, an assumption which (as was pointed out [12]) is not generally valid. The evolution of the cavity size distribution was evaluated numerically using an approach that was analogous to that used here.

It is a common experience in sintering and hot isostatic pressing to observe that it is difficult to achieve full density. This is in marked contrast to the predictions of rapid and complete densification obtained from standard models derived under the assumptions of diffusional control and a single pore size. We have shown that more realistic results may be obtained by assuming that a distribution of pore sizes exists in the material. We have also shown that the most likely pore size can increase even as densification proceeds and all pores shrink.

It is beyond the scope of this paper to relate pore size distributions to particle size distributions and particle packings. However, it is clear from this work that behaviour in the limit of long time (and high density) is controlled by large pores. It is expected that these large pores would be found near large initial particles or fully densified agglomerates.

Appendix; alternative derivation of Equation 15

In this Appendix we present an alternative derivation of Equation 15, one that is perhaps simpler than that developed in the text, but which nevertheless is mathematically rigorous.

Consider a pore that has size ϱ_0 at time τ_0 and size $\varrho \geqslant 0$ at some later time τ. The relationship between ϱ and τ is given by Equation 10 (dropping the prime symbol in Equation 10). Likewise, consider another pore that has size $\varrho_0 + d\varrho_0$ at time τ_0 and size $\varrho + d\varrho$ at time τ. For this case, Equation 10 becomes

$$\tau - \tau_0 = \int_{\varrho_0+d\varrho_0}^{\varrho+d\varrho} \frac{d\varrho}{v(\varrho)} \quad (A1)$$

Subtracting Equation 10 from Equation A1,

$$0 = \int_{\varrho_0+d\varrho_0}^{\varrho+d\varrho} \frac{d\varrho}{v(\varrho)} - \int_{\varrho_0}^{\varrho} \frac{d\varrho}{v(\varrho)} \quad (A2)$$

or

$$\int_{\varrho_0+d\varrho_0}^{\varrho+d\varrho} \frac{d\varrho}{v(\varrho)} = \int_{\varrho_0}^{\varrho} \frac{d\varrho}{v(\varrho)} \quad (A3)$$

For infinitesimally small $d\varrho_0$ and $d\varrho$, Equation A3 can be expressed as

$$\frac{d\varrho}{v(\varrho)} = \frac{d\varrho_0}{v(\varrho_0)} \quad (A4)$$

The concentration of pores at time τ_0 within the interval ϱ_0 to $\varrho_0 + d\varrho_0$ is $f(\varrho_0, \tau_0)d\varrho_0$ and that at time τ within the interval ϱ to $\varrho + d\varrho$ is $f(\varrho, \tau)d\varrho$. Clearly, these must be equal, i.e.

$$f(\varrho, \tau)d\varrho = f(\varrho_0, \tau_0)d\varrho_0 \quad (A5)$$

Eliminating $d\varrho$ and $d\varrho_0$ from Equation A5 by application of Equation A4, we find that

$$v(\varrho)f(\varrho, \tau) = v(\varrho_0)f(\varrho_0, \tau_0) \quad (A6)$$

and we see that Equations A6 and 15 are identical.

Acknowledgement

Support of this work by the United States Air Force Office of Scientific Research under Grant No. 82-0238 is gratefully acknowledged.

References

1. A. J. MARKWORTH, *Scripta Metall.* **18** (1984) 1309.
2. G. W. GREENWOOD, in "Vacancies '76", edited by R. E. Smallman and J. E. Harris (The Metals Society, London, 1977) p. 141.
3. Ya. E. GEGUZIN and I. M. LIFSHITS, *Soviet Phys. – Solid State* **4** (1962) 971.
4. A. J. MARKWORTH, *Scripta Metall.* **6** (1972) 957.
5. H. TRINKAUS, *ibid.* **15** (1981) 825.
6. D. HULL and D. E. RIMMER, *Phil. Mag.* **4** (1959) 673.
7. J. WEERTMAN, *Scripta Metall.* **7** (1973) 1129.
8. A. D. RANDOLPH and M. A. LARSON, "Theory of Particulate Processes – Analysis and Techniques of Continuous Crystallization" (Academic Press, New York, 1971) pp. 53 ff.
9. A. J. MARKWORTH, in "Defects and Transport in Oxides", edited by M. S. Seltzer and R. I. Jaffee (Plenum Press, New York, 1974) p. 397.
10. G. TOMANDL, in "Science of Ceramics", Vol. 9, edited by K. J. deVries (The Netherlands Ceramic Society, Tiel, 1977) p. 158.
11. G. SOULLARD, L. MARTINEZ and J. OSEGUERA, *Scripta Metall.* **19** (1985) 581.
12. L. MARTINEZ and J. H. SCHNEIBEL, *Phil. Mag. A* **51** (1985) L29.

Received 17 February
and accepted 2 June 1986